arXiv:1007.1063v1 [cond-mat.dis-nn] 7 Jul 2010

Angular rigidity in tetrahedral network glasses

M. Bauchy[1], M. Micoulaut[1], M. Celino[2] and C. Massobrio[3]
[1] *Laboratoire de Physique Théorique de la Matière Condensé, Université Pierre et Marie Curie, Boite 121, 4, Place Jussieu, 75252 Paris Cedex 05, France*
[2] *ENEA, Ente per le Nuove Tecnologie, l'Energia e l'Ambiente, Unite Materiali e Nuove Tecnologie, C.R. Casaccia, CP 2400, 00100 Roma, Italy*
[3] *Institut de Physique et de Chimie des Matériaux de Strasbourg, 23 rue du Loess, BP43, F-67034 Strasbourg Cedex 2, France*
(Dated: July 8, 2010)

A set of oxide and chalcogenide tetrahedral glasses are investigated using molecular dynamics simulations. It is shown that unlike stoichiometric selenides such as $GeSe_2$ and $SiSe_2$, germania and silica display large standard deviations in the associated bond angle distributions. Within bond-bending constraints theory, this pattern can be interpreted as a manifestation of *broken* (i.e. ineffective) oxygen bond-bending constraints. The same analysis reveals that the changes in the Ge composition affects mostly bending around germanium in binary Ge-Se systems, leaving Se-centred bending almost unchanged. In contrast, the corresponding Se twisting (quantified by the dihedral angle) depends on the Ge composition and is reduced when the system becomes rigid. Our results establishes the atomic-scale foundations of the phenomelogical rigidity theory, thereby profoundly extending its significance and impact on the structural description of network glasses.

PACS numbers: 61.43.Fs

The large variety of physico-chemical behaviours inherent in tetrahedral network glasses (in particular, those involving Group IV (A=Si, Ge) oxides (X=O) or chalcogenides (X=S,Se,Te)) is deeply related to the underlying network topology, i.e. the nature of the connections (edge- or corner-sharing) among the basic tetrahedral structural units [3, 4]. In the search of an unifying approach, it is tempting to follow rigidity theory, that describes the interplay between network properties and connectivity by considering covalent networks in very much the same fashion as mechanical trusses [5]. This is achieved via enumeration of mechanical rigid constraints n_c arising from relevant atomic interactions, $r/2$ bond-stretching (radial) and $(2r-3)$ bond-bending (angular) for a r-folded atom. As a consequence, a rigidity transition at the network mean coordination number $\bar{r}$=2.4 is identified [5], separating underconstrained networks having low-frequency (floppy) deformation modes ($n_c < 3$) from overconstrained ones ($n_c > 3$).

Accordingly, all stoichiometric compounds AX_2 should be stressed rigid i.e. they have more constraints than degrees of freedom (n_c=3.67), with a mean coordination number of $\bar{r}$=2.67 larger than the critical $\bar{r}_c$=2.4 for which optimal glass formation with small enthalpic changes at the glass transition, is supposed to occur [6].

The legitimacy of such a picture is challenged by the observation that silica (SiO_2) and germania (GeO_2) are found to form rather easily glasses [7], in contrast with the corresponding chalcogenides (e.g. $GeSe_2$) found at the very limit of the binary glass-forming region (in e.g. Ge_xSe_{1-x} [8]). Furthermore, oxides have a low frequency (floppy) contribution in the vibrational density of states, suggesting that these systems are flexible [9] or, at least, nearly optimally constrained [10] (isostatic, n_c=3). The latter result can be recovered in rigidity theory under the heuristic assumption that enhanced oxygen bond-angle values lead to *broken* angular constraints [11] reducing n_c from 3.67 to 3.0. However, a microscopic scale rationale for this specific network behavior is lacking.

These pieces of evidence call for the basic assertions of rigidity theory, when applied to the above oxide and chalcogenide networks, to be revisited. Here we rely on an atomic-scale approach (as molecular dynamics) able to substantiate and enrich the general trends of rigidity theory via the explicit account of the details of chemical bonding.

In this Letter we bridge the gap between constraint counting algorithms and the statistical mechanical behavior of relevant atomic-scale quantities (angular distributions) by considering a set of chalcogenides and oxide glasses. Two issues commonly tackled within rigidity theory are given new atomic-scale foundations. First, by focussing on the stoichiometric AX_2 composition (i.e. SiO_2, GeO_2, $SiSe_2$ and $GeSe_2$) we show that oxide systems contain tetrahedra which act as rigid units having a much smaller minimal angular excursion (quantified by σ_θ, the standard deviation of the partial bond angle distributions) than their chalcogenide counterparts. By analysing in a similar fashion the binary Ge_xSe_{1-x} system with changing compositions, we find that changes in rigidity (increasing Ge content x) are noticeable in the angular environment of germanium, leaving the Se centred angular excursions nearly unchanged when moving from a flexible to a stressed rigid phase. It appears that the amplitude of the angular distribution around A atoms is increased in the stressed rigid phase with an increased distorsion (i.e. higher σ_θs) of the tetrahedra. This result allows reconsidering the general accepted pic-

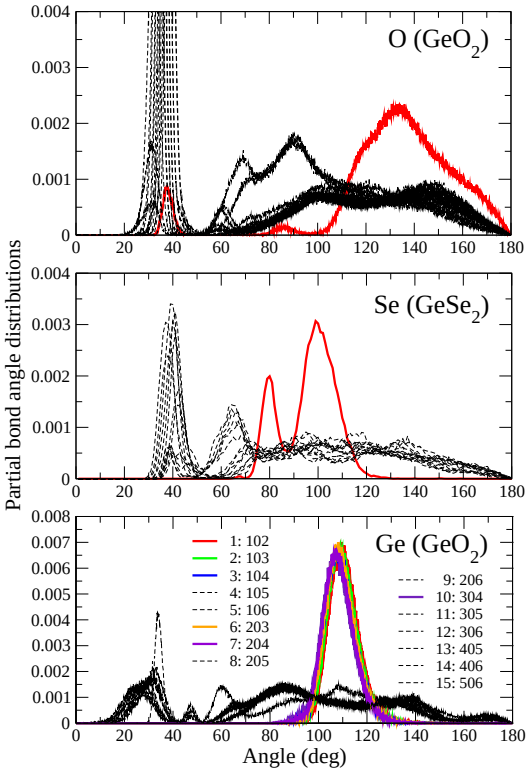

FIG. 1: (color online) From top to bottom: oxygen, selenium and germanium partial bond angle distributions (PBAD) in GeO_2 and $GeSe_2$ for an arbitrary N=6. The colored curves correspond to PBADs having the lowest standard deviation(s) σ_θ (see Fig. 2). The sharp peaks at $\theta \simeq 40^o$ correspond to the hard-core repulsion. Labels defined in the bottom panel are used throughout the text.

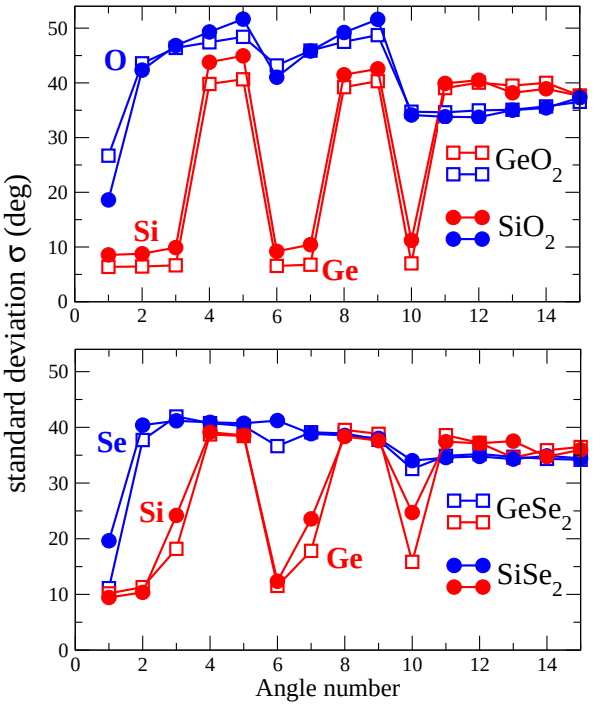

FIG. 2: (color online) Standard deviation $\sigma_{\theta_{ij}}$ of partial bond angle distributions (PBADs) in oxides (SiO_2, GeO_2, top panel) and chalcogenides ($SiSe_2$, $GeSe_2$, bottom panel) as a function of the angle number (see defintion in Fig. 1).

ture of a Ge-Se network made of flexible Se-chains and rigid $GeSe_{4/2}$ tetrahedra [5]. As a second main outcome, we find that σ_θ for oxygen in oxides, is much larger than σ_θ for selenium in $GeSe_2$, proving that oxygen bending constraints are *broken* (i.e. ineffective) in SiO_2 and GeO_2. This provides a microscopic rationale for the sensitivity to bond-bending around oxygen in oxide networks, consistent with experimental evidence [11].

Our analysis is based on molecular dynamics trajectories obtained at T=300 K for a set of glassy systems encompassing GeO_2, SiO_2, $SiSe_2$ and Ge_xSe_{1-x} for 4 different compositions: $x = 0.10$ ($GeSe_9$ in the flexible phase), $x = 0.20$ ($GeSe_4$ at the rigidity transition [6]), $x = 0.25$ ($GeSe_3$ in the intermediate phase [8]) and $x = 0.33$ ($GeSe_2$ in the stressed rigid phase). Oxides at the experimental densities have been simulated according to Ref. [12] and [13] using a classical Born-Mayer force field. Due to the large difference of electronegativity between Si(Ge) and O, this choice ensures plausible qualitative modelling within classical molecular dynamics. In the case of $SiSe_2$ and Ge_xSe_{1-x} systems, we resort to first-principle molecular dynamics (FPMD) within a fully self-consistent framework that proved adequate to describe chemical bonding and its changes with concentration. For some of the systems, temporal trajectories recorded previously are substantially extended to attain optimal statistical accuracy (within a few percent at most). Otherwise, as in the case of $GeSe_9$ and $GeSe_3$, glassy structures are produced from the outset after cooling from the liquid state and appropriate structural relaxation. Overall, typical time trajectories for collection of the averages in the glassy state cover ~ 100 ps. Details on the FPMD methodology and the productions of glassy structure are extensively reported in [14] and [15]. For all glassy structures, the atomic-scale picture is consistent with that obtained by using an alternative first-principles approach [16].

To obtain the number of bond-stretching interactions we have focused on neighbour distribution functions (NDFs). A set of NDFs can be defined by fixing the neighbor number n (first, second etc), the sum of all

NDFs yielding the standard pair distribution function $g_i(r)$ (i=A,X). Integration of $g_i(r)$(i=A,X) up to the first minimum gives the coordination numbers r_X and r_A, and hence the corresponding number of bond-stretching constraints $r_i/2$ (i=A,X). For all considered systems, we find $r_X = 2$ and $r_A = 4$ leading to 1 and 2 bond-stretching constraints for the X and A atoms. For instance, when integrating the pair distribution function up to its first minimum, we find for GeO_2 r_{Ge}=4.01 and r_O=1.97, and for $GeSe_2$, r_{Ge}=4.02 and r_{Se}=1.96, in agreement with experiments [4, 17, 18].

Bond-bending constraint counting is based on partial bond angle distributions (PBADs) $P(\theta_{ij})$ defined as follows: for each type of central atom 0, the N first neighbours i are selected and the N(N-1)/2 corresponding angles $i0j$ (i=1..N-1, j=2..N) computed, i.e. 102, 103, 203, etc. The standard deviation $\sigma_{\theta_{ij}}$ of the distribution $P(\theta_{ij})$ gives a quantitative estimate about the angular excursion around a mean angular value, and provides a measure of the bond-bending strength (small values, i.e. intact bond-bending constraint) or the bond-bending weakness (large values, ineffective or *broken* constraint).

Figure 1 shows such PBADs for oxygen (Ge-O-Ge angle) and germanium (O-Ge-O) in GeO_2 and for selenium (Ge-Se-Ge) in $GeSe_2$ for an arbitrary N=6 leading to 15 possible PBAD's. Oxygen displays for the principal contribution 102 (angle number 1, in red) a broad distribution centred around the angle $\theta = 135^o$, corresponding to the one defined by the two closest (Ge) neighbours of oxygen, in agreement with experiments [19]. Secondary distributions 103 and 203 show peaks centred at around $\theta \simeq 90^o$ and 75^o. In contrast, $GeSe_2$ exhibits a much sharper distribution for the same 102 contribution, implying reduced angular excursions as compared to GeO_2. The contributions to the bimodal $GeSe_2$ distribution at 80^o and 100^o can be respectively assigned to edge-sharing and corner-sharing tetrahedra [20], a feature that is absent in oxides. Six germanium centred angles (bottom panel) are found to have almost the same distribution in GeO_2, centred at an angle of 109^o typical of the tetrahedral environment.

The behavior of the standard deviations for the PBADs is shown in Fig. 2, where, for sake of simplicity, each PBAD is given a distinct number (see bottom part of Fig. 1 for the definition). For all chalcogenide or oxide systems, the PBADs relative to the Group IV (Si, Ge) atom have a low standard deviation $\sigma_{\theta_{ij}}$, of the order of 10-20^o, for instance $\sigma_{\theta_{ij}} \simeq 7^o$ for the 102 PBAD of GeO_2. These values are much smaller than those of the other distributions (105, 106, etc.), found close at $\simeq 40^o$. In addition to very low angular excursions around the tetrahedral angle of 109^o (Fig. 2 top), oxides feature all $\sigma_{\theta_{ij}}$ (i,j<4) nearly equal for the six relevant (Ge,Si) distributions. A different situation occurs in stoichiometric chalcogenides (Fig. 2 bottom, red curve) which exhibit increased bending for the angles defining the tetrahedra (angle 3: 104, angle 7: 204, etc.). These results exemplifies the difference in the bending nature of the tetrahedra in these two families of networks, pointing to a higher rigidity of the tetrahedra in oxides, as all anglular excursions are maintained at the same low value (typically 7^o).

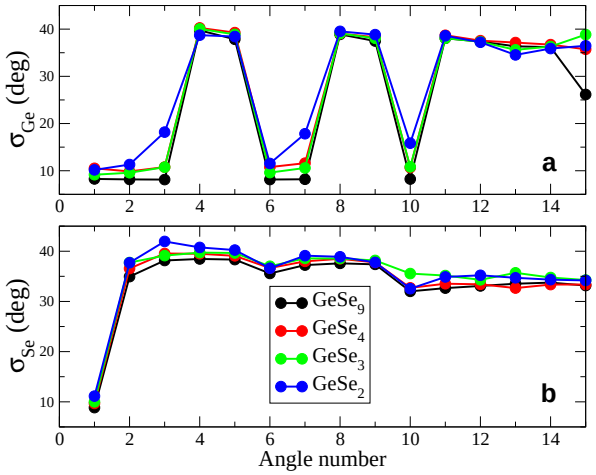

FIG. 3: (color online) Standard deviation σ_{Ge} and σ_{Se} extracted from the partial bond angle distributions (PBAD) for four selected compositions in glassy Ge_xSe_{1-x}

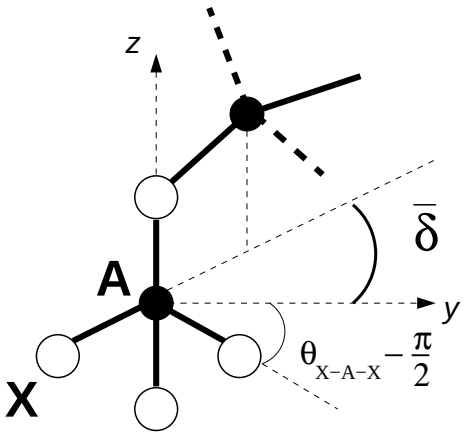

FIG. 4: Definition of the dihedral angle $\bar{\delta}$ used in the text. Note that the upper black-filled atom can X (r_X=2) or A (r_A=4).

Angle distributions around the Group VI atoms are markedly different. Indeed, the selenium standard deviation $\sigma_{\theta_{12}}$ (angle number 1) is found to be low (11.7^o for $GeSe_2$) compared to the corresponding oxide system (26.7^o for GeO_2). Therefore, the restoring effect associated with bending is much lower in GeO_2, allowing for the identification of a *broken* angular constraint. One should also have in mind that the standard deviations found around 20^o are close to those found in high temperature liquids (18-25^o at 1373 K for $GeSe_2$), where angular constraints are assumed to be broken [21]. This re-

System	SiO_2	GeO_2	$SiSe_2$	$GeSe_9$	$GeSe_4$	$GeSe_3$	$GeSe_2$
$\bar{\delta}$(deg)	30.9	30.4	30.9	35.0	40.3	31.9	30.6
σ_δ(deg)	17.7	17.5	23.9	27.4	25.9	20.6	21.6

TABLE I: Mean dihedral angle $\bar{\delta}$ and standard deviation σ_δ of the dihedral angle distribution for the seven investigated systems

.

duces the number density of constraints to n_c=0.33($\frac{5}{2}r_A$-3)+0.67($\frac{5}{2}r_X$-4)=3.00, i.e. oxides are optimally constrained. Because of its large fraction of ES tetrahedra [15], the situation of $SiSe_2$ appears to be somewhat intermediate with $\sigma_{\theta_{12}}$=19.6^o, resulting from contributions arising from both ES and CS tetrahedra which have respectively ineffective and intact Se bond-bending constraints.

It is of interest to apply the above rationale to the Ge_xSe_{1-x} family of systems, since both the elastic nature (flexible, rigid) and the connectivity are strongly dependent on composition. By increasing the Ge concentration the angular excursion inside the tetrahedra is seen to increase (e.g. σ_{Ge} moving up to 20^o from less than 10^o in the n=3 (104) PBAD) while leaving the stiffest angle (102) constant. On the other hand, bending around the Se atoms is nearly unchanged and it does not display any noticable change when the system becomes rigid. To find a structural parameter pertaining to the Se atoms and sensitive to changes in composition, we have to resort to the dihedral angle $\bar{\delta}$ around a Se atom (see definition in Fig. 4). As shown in Table I, the dihedral angular excursion takes a value of σ_δ=27.4^o for the flexible $GeSe_9$ composition and decreases significantly (down to 20^o-21^o) for the compositions of rigid systems $GeSe_3$ and $GeSe_2$. Therefore, the network adapts to the predominant presence of Se atoms both by decreasing the angular variability inside the $GeSe_{4/2}$ tetrahedra, and by allowing for enhanced twisting along the Se chains. Finally, in view of the behaviour of σ_A (A=O,Se) from both Figs. 2 and 3, it becomes clear that the angular motion inside SiO_2 and GeO_2 tetrahedra behaves very similarly to flexible $GeSe_9$ or optimally constrained $GeSe_4$ and $GeSe_3$ networks. On the other hand, these oxide systems definitely contrast with the corresponding stressed rigid chalcogenides $SiSe_2$ and $GeSe_2$.

We showed that structural information gathered from molecular dynamics is able to provide an atomic-scale counterpart to phenomenological constraint counting concepts applied to network glasses. This leads to a clear picture of the topological differences between systems having the same composition but different chemical nature and systems made of the same species but differing in composition. The differences between glasses (oxides and chalcogenides) of same stoichiometry are rationalized in terms of amplitude of the inter- and intratetrahedral bending angular variations. In oxides, the results show increased bending aroud the oxygen atom, consistent with a direct Maxwell constraint counting and the non-stressed rigid nature of these glasses. In systems undergoing a rigidity transition (e.g. Ge_xSe_{1-x}), it is found that the angles defining the $GeSe_{4/2}$ tetrahedron soften with decreasing Ge weight while the Se angular bending is almost unchanged. Flexibility along the Se chains is best accounted for in terms of twisting along the Se chains, found to increase with Se content. The present approach finally provides a general framework for establishng bonding constraints in a neat way via model simulations, and should be used in the future for establishing constraint counting algorithms in more complex glassy materials.

It is a pleasure to acknowledge ongoing discussions with Christophe Bichara, Punit Boolchand and Jean-Yves Raty. This work has been supported by Agence Nationale de la Recherche (ANR) n.09-BLAN-0190-01. The calculations were performed at the IDRIS computer center of CNRS and at the Computer Center DSI of UPMC (France).

[1] *Insulating and Semiconducting glasses*, P. Boolchand Ed., World Scientific (Singapore, 2001).
[2] P. Richet and B. O. Mysen, *Silicate Glasses and Melts: Properties and Structure* (Elsevier, Amsterdam, 2005).
[3] M. Wilson, P.S. Salmon, Phys. Rev. Lett. **103**, 157801 (2009).
[4] P.S. Salmon, Proc. R. Soc. A **445**, 351 (1994).
[5] *Rigidity theory and applications*, M.F. Thorpe and P.M Duxbury Eds. (Kluwer Academic, Plenum Publishers New York, 1999).
[6] J.C. Phillips, J. Non-Cryst. Solids **34**, 153 (1979) ; M.F. Thorpe, J. Non-Cryst. Solids **57**, 355 (1983).
[7] M.C. Weinberg, D.R. Uhlmann and E.D. Zanotto, J. Am. Ceram. Soc. **72**, 2054 (1989).
[8] P. Boolchand, X. Feng and W.J. Bresser, J. Non-Cryst. Solids **293**, 248 (2001).
[9] K. Trachenko, M.T. Dove, V. Brazhkin, and F.S. El'kin, Phys. Rev. Lett. **93**, 135502 (2004).
[10] M. Wyart, Ann. Phys. **30**, 1 (2005).
[11] M. Zhang and P. Boolchand, Science **266**, 1355 (1994).
[12] M. Micoulaut, Y. Guissani and B. Guillot, Phys. Rev. E **73** 031504 (2006)
[13] B. Guillot and Y. Guissani, J. Chem. Phys. **104**, 7633 (1996).
[14] C. Massobrio, M. Micoulaut, P.S. Salmon, Solid State Sci. **12**, 199 (2010)
[15] M. Celino and C. Massobrio, Phys. Rev. Lett. **90**, 125502 (2003).
[16] D. Tafen and D. A. Drabold, Phys. Rev. B**71**, 054206 (2005).
[17] R.W. Johnson, J. Non-Cryst. Solids **88**, 386 (1986).
[18] P.S. Salmon, A.C. Barnes, R.A. Martin and G.J. Cuello,

J. Phys. Cond. Matt. **19**, 415110 (2007).
[19] R. Hussein, R. Dupree and D. Holland, J. Non-Cryst. Solids **246**, 159 (1999).
[20] C. Massobrio and A. Pasquarello, Phys. Rev. B**77**, 144207 (2008).
[21] P.K. Gupta and J.C. Mauro, J. Chem. Phys. **130**, 094503 (2009).